Genetic, biochemical, and molecular characterization of *Methanosarcina barkeri* mutants lacking three distinct classes of hydrogenase

Thomas D. Mand,[a] Gargi Kulkarni,[a]* William W. Metcalf[a]#

[a]Department of Microbiology, University of Illinois at Urbana-Champaign, Urbana, Illinois, USA

Running Head: Analysis of *M. barkeri* hydrogenase mutants

#Address correspondence to William W. Metcalf, metcalf@life.illinois.edu.

*Present address: Gargi Kulkarni, California Institute of Technology, Pasadena, California, USA

T.D.M. and G.K. contributed equally to this work.

ABSTRACT

The methanogenic archaeon *Methanosarcina barkeri* encodes three distinct types of hydrogenase, whose functions vary depending on the growth substrate. These include the F420-dependent (Frh), methanophenazine-dependent (Vht), and ferredoxin-dependent (Ech) hydrogenases. To investigate their physiological roles, we characterized a series of mutants lacking each hydrogenase in various combinations. Mutants lacking Frh, Vht, or Ech in any combination failed to grow on H_2/CO_2, whereas only Vht and Ech were essential for growth on acetate. In contrast, a mutant lacking all three grew on methanol with a final growth yield similar to wild-type, produced methane and CO_2 in the expected 3:1 ratio, but had a *ca.* 33% slower growth rate. Thus, hydrogenases play a significant, but non-essential, role during growth on this substrate. As previously observed, mutants lacking Ech fail to grow on methanol/H_2 unless supplemented with biosynthetic precursors. Interestingly, this phenotype was abolished in the Δ*ech*/Δ*frh* and Δ*ech*/Δ*frh*/Δ*vht* mutants, consistent with the idea that hydrogenases inhibit methanol oxidation in the presence of H_2, which prevents production of reducing equivalents needed for biosynthesis. Quantification of methane and CO_2 produced from methanol by resting cell suspensions of various mutants supports this conclusion. Based on global transcriptional profiles, none of the hydrogenases are upregulated to compensate for loss of the others. However, transcript levels of the F420 dehydrogenase operon were significantly higher in all strains lacking *frh*, suggesting a mechanism to sense the redox state of F420. The roles of the hydrogenases in energy conservation during growth with each methanogenic pathway are discussed.

40

41 **IMPORTANCE**

42 Methanogenic archaea are key players in the global carbon cycle due to their
43 ability to facilitate the remineralization of organic substrates in many anaerobic
44 environments. The consequences of biological methanogenesis are far reaching,
45 with impacts on atmospheric methane and CO_2 concentrations, agriculture, energy
46 production, waste treatment and human health. The data presented here clarify the
47 *in vivo* function of hydrogenases during methanogenesis, which in turn deepens our
48 understanding of this unique form of metabolism. This knowledge is critical for a
49 variety of important issues ranging from atmospheric composition to human health.

50

51 **INTRODUCTION**

52 The ability to metabolize molecular hydrogen (H_2) is a key metabolic feature
53 in methanogenic Archaea (1). This trait is conferred by a class of enzymes known as
54 hydrogenases, which catalyze the reversible oxidation of H_2 coupled to various
55 electron donors/acceptors (2, 3). At least five distinct types of hydrogenases are
56 found in methanogenic archaea. These enzymes differ with respect to their redox
57 partners, their cellular localization, and whether their activity is linked to
58 production or consumption of membrane potential (4). Biochemical
59 characterization of these diverse hydrogenases led to proposed functions for each
60 enzyme class that differ substantially between methanogens with and without
61 cytochromes (5).

Methanogens without cytochromes produce at least four types of hydrogenase; including (*i)* the electron-bifurcating Mvh hydrogenase, which couples oxidation of hydrogen to reduction of ferredoxin and a mixed coenzyme M-coenzyme B disulfide, (*ii)* the coenzyme F420-dependent hydrogenase, (*iii)* the [Fe] hydrogenase, which couples hydrogen oxidation to reduction of methenyltetrahydromethanopterin, and (*iv)* the ferredoxin-dependent, energy-converting hydrogenases (4). The first three are cytoplasmic enzymes, which supply the electrons needed to reduce CO_2 to methane. The last is a membrane bound multi-subunit complex that couples hydrogenase activity to the production/consumption of the ion-motive force across the cell membrane (hence the designation as "energy-converting"). In non-cytochrome-containing methanogens, these energy-converting hydrogenases are believed to provide low-potential electrons, in the form of reduced ferredoxin, needed for anaplerotic reactions (6).

Methanogens with cytochromes, typified by *Methanosarcina barkeri*, encode a different set of hydrogenases that includes one cytoplasmic and two membrane-bound enzymes (Fig 1) (7). Like the non-cytochrome containing methanogens, *M. barkeri* produces a cytoplasmic, three-subunit F_{420}-dependent hydrogenase known as Frh (for F420-reducing hydrogenase). Frh is encoded by the four-gene *frhADGB* operon, which encodes the α, β and γ subunits (FrhA, FrhB and FrhG, respectively), along with the maturation protease FrhD (8). A second locus, *freAEGB*, encodes proteins that are 86-88% identical to FrhA, FrhB and FrhG, but lacks the gene for the maturation protease FrhD, instead encoding a small protein of unknown function

(FrhE). It is not known whether the *fre* operon is capable of producing an active hydrogenase (8-11). A membrane-bound hydrogenase linked to the quinone-like electron carrier methanophenazine has, to date, been found only in *Methanosarcina* species. This enzyme, known as Vht because it was initially identified as a viologen-reducing hydrogenase, is encoded by the *vhtGACD* operon, which encodes the biochemically characterized enzyme comprised of VhtA and VhtG, along with a putative membrane-bound cytochrome, VhtC, that does not co-purify with the active enzyme, and a maturation protease, VhtD (7). As with the F420-reducing hydrogenase, a second locus that lacks the maturation protease is encoded in *M. barkeri* strains. This operon (*vhxGAC*) encodes proteins that display *ca.* 50% amino acid identity with those encoded by *vhtGACD.* Like *freAEGB*, it is not known whether the *vhx* operon produces an active hydrogenase (7). Finally, *M. barkeri* encodes a membrane-bound, ferredoxin-dependent energy-converting hydrogenase (Ech) (12). This five-subunit enzyme complex is much simpler than, and only distantly related to, the energy-converting hydrogenases of the non-cytochrome methanogens, which typically contain more than a dozen subunits (3). Homologs of the electron bifurcating- and methenyltetrahydromethanopterin-reducing hydrogenases are not known to occur in cytochrome-containing methanogens.

A key difference between the cytochrome-containing and non-cytochrome-containing methanogens is the ability of the former to use one-carbon (C-1) compounds and acetic acid, in addition to H_2/CO_2, as growth substrates. Catabolism of these chemically diverse substrates involves four distinct methanogenic pathways: the CO_2 reduction pathway, the methyl reduction pathway, the

methylotrophic pathway and the aceticlastic pathway (13, 14). While several of these pathways share common steps, they differ substantially with respect to involvement of key enzymes and the direction of metabolic flux during methane production (Fig 2). Surprisingly, it now appears that some *Methanosarcina* species (*e.g. M. barkeri*) use hydrogenases in each of the four pathways, regardless of whether external H_2 is provided as a growth substrate (15).

During the CO_2 reduction pathway, wherein CO_2 is reduced to CH_4 in a stepwise manner, hydrogenases produce the electron-donating cofactors required for four distinct reduction steps (Fig 2) (5). Initial reduction of CO_2 to formyl-methanofuran requires reduced Fd (Fd_{red}), which is produced by Ech. This reaction is dependent on ion-motive force because reduction of Fd by H_2 is endergonic under physiological conditions (16). Subsequent reduction of methenyl-tetrahydrosarcinapterin (H_4SPT) to methylene-H_4SPT, and of methylene-H_4SPT to methyl-H_4SPT, requires reduced coenzyme F420 ($F420_{red}$), which is supplied by Frh. Finally, reduction of a methyl group to methane using coenzyme B produces a heterodisulfide of coenzyme M and coenzyme B (CoM-S-S-CoB), which must be reduced to produce the free CoM and CoB needed for continued methanogenesis. This reaction is catalyzed by a membrane bound heterodisulfide reductase (HdrED), which uses the reduced form of a membrane-bound cofactor, methanophenazine, as the source of electrons (17). H_2, in turn, serves as the reductant for generation of reduced methanophenzaine via membrane-bound Vht hydrogenase. Thus, all three types of hydrogenase are predicted to be required for growth via CO_2 reduction, a

130 conclusion that has been validated by the phenotypic analysis of single mutants (11,
131 15, 16).

132 In contrast, methanogenesis via the methyl reduction pathway is expected to
133 require only Vht. In this pathway, methyl-CoM derived from C-1 compounds, such as
134 methanol or methylamines, is directly reduced to methane using CoB as the electron
135 donor. As with the CO_2 reduction pathway, this produces a CoM-S-S-CoB disulfide
136 that must be regenerated in a pathway requiring HdrDE and reduced
137 methanophenazine, which is presumably generated by Vht (Fig 2). This idea is
138 supported by the analysis of conditional *vht* mutants (15). Neither Frh nor Ech is
139 required for methanogenesis in this model, a finding that is consistent with
140 experimental data from Δ*frh* and Δ*ech* mutants (11, 16). Nevertheless, the *M. barkeri*
141 Δ*ech* strain cannot grow via the methyl reduction pathway unless the media are
142 supplemented with acetate and/or pyruvate. Thus, Ech plays an essential
143 biosynthetic role under these conditions, which is probably the H_2-dependent
144 synthesis of reduced ferredoxin needed for synthesis of acetyl-CoA and pyruvate
145 (16).

146 During aceticlastic methanogenesis, both the Ech and Vht hydrogenases play
147 a critical role in methanogenesis. In this pathway, acetyl-CoA is split into methyl-
148 H_4SPT and enzyme-bound [CO] by the acetyl-CoA decarbonylase/synthase (ACDS)
149 enzyme complex. CO is then further oxidized to CO_2 with concomitant reduction of
150 ferredoxin (12, 16). It is believed that the exergonic oxidation of ferredoxin by Ech
151 produces H_2 and contributes to the proton motive force by transferring protons
152 across the membrane. The proton motive force is further enhanced by a putative H_2

153 cycling mechanism, in which the H_2 produced by Ech diffuses across the membrane,
154 where it is oxidized by Vht to produce reduced methanophenazine. This unusual
155 electron transport chain is completed when the reduced methanophenazine
156 produced by Vht is used by HdrDE to regenerate free CoM and CoB from the CoM-S-
157 S-CoB heterodisulfide (Fig 2) (18). Participation of these hydrogenases in the
158 aceticlastic pathway is supported by mutagenic studies showing that *ech* and *vht*
159 mutants do not grow with acetate as the sole substrate, regardless of whether
160 biosynthetic precursors were supplied (15, 16).

161 Finally, all three types of hydrogenases are thought to be involved in
162 methylotrophic methanogenesis via a H_2 cycling mechanism similar to that
163 described for aceticlastic growth (15). In this pathway, $F420_{red}$ and Fd_{red}, produced
164 by the stepwise oxidation of methyl groups to CO_2, are converted to molecular H_2 by
165 Frh and Ech, respectively (Fig 2). H_2 then diffuses to the outer surface of the cell
166 membrane where it is oxidized by Vht, releasing protons on the outside of the cell
167 and contributing to the generation of an ion-motive force (Fig 3) (15). Nevertheless,
168 *M. barkeri* Δ*frh* and Δ*ech* strains are capable of methylotrophic growth, indicating
169 the presence of alternative pathways for transfer of electrons from $F420_{red}$ and Fd_{red}
170 to the electron transport chain (11, 16). The membrane-bound F420 dehydrogenase
171 complex (Fpo) has been identified as the alternate mechanism of electron transfer
172 from $F420_{red}$ (11). This enzyme couples the exergonic reduction of
173 methanophenazine by $F420_{red}$, with the generation of proton motive force in a H_2
174 independent manner. However, the *M. barkeri* Δ*frh* strain exhibits slower growth
175 rates than wild type *M. barkeri*, showing that the H_2-independent electron transport

chain is less effective than electron transport via H_2 cycling. The observation that Δ*fpo*/Δ*frh* double mutants are incapable of methylotrophic growth shows that additional electron transport routes are either not present, or not sufficient for methylotrophic growth (11). Mutants lacking Vht are inviable under all growth conditions, including methylotrophic growth, unless Frh is also removed. This phenotype is probably due the inability to recapture H_2 produced in the cytoplasm, which causes redox imbalance and cell lysis (15).

Although the three *M. barkeri* hydrogenases have been studied *in vitro* and in certain mutants, a complete analysis of their role during growth on various substrates has yet to be reported. In this study, all five hydrogenase operons were systematically deleted in all viable combinations, and the physiological ramifications of these mutations examined by measuring growth, methanogenesis and hydrogenase activity on various growth substrates. We also performed global transcriptional profiling to assess the possibility that alternate electron transport chain components might be upregulated to compensate for the loss of specific hydrogenases. The data suggest that hydrogenases are not required for methylotrophic methanogenesis, but are essential for CO_2 reductive, methyl reductive, and acetoclastic methanogenesis. Additionally, an inhibitory effect of H_2 on the methyl oxidative pathway appears to be mediated by all three hydrogenases.

RESULTS

Construction of hydrogenase deletion mutants. To assess the role of the *M. barkeri* hydrogenases during growth on various substrates, we constructed mutants

lacking the *frhADGB*, *freAEGB*, *vhtGACD*, *vhxGAC* and *echABCDEF* operons, individually and in all possible combinations (Fig S1). Because mutants lacking *vht* are only viable in Δ*frh* mutants (15), we also created a series of conditional mutants that have the *vht* promoter replaced by the synthetic P_{tet} promoter, which is expressed in the presence of tetracycline and tightly repressed in its absence (19). To simplify the isolation of strains lacking the adjacent *vht* and *vhx* loci, we constructed a mutant allele (denoted Δ*vht-vhx*) that deleted both operons along with two intervening genes that encode a putative peptidoglycan binding protein (Mbar_A1842) and an uncharacterized hypothetical protein (Mbar_A1843). The full set of strains containing deletions for hydrogenase operons in all possible combinations were successfully generated and verified by either Southern hybridization or PCR (Figures S2-S5).

Characterization of growth phenotypes in hydrogenase deletion mutants. The generation time, growth yield and duration of lag phase for each mutant was determined by monitoring optical density during growth in a variety of media, providing clues as to the function of each hydrogenase during utilization of various carbon and energy sources (Table 1). With the exception of the Δ*fre* and Δ*vhx* mutations, which had no discernable phenotypes alone or in combination with other gene deletions, each of the mutations caused significant growth defects in one or more media.

Strains containing the Δ*ech* mutation were unable to grow in either H_2/CO_2 or acetate media, regardless of whether the other hydrogenase genes were deleted. However, with the exception of the P_{tet}*vht*/Δ*ech* mutant discussed below, these

mutants all grew on methanol medium, albeit with reduced growth rates. Consistent with previous reports (16), the Δ*ech* single mutant was unable to grow on unsupplemented methanol/H_2/CO_2 medium. Interestingly, the Δ*ech*/Δ*frh* double mutant regained the ability to grow in this medium, but with diminished rate and yield and the longest lag phase observed in any of our experiments. These phenotypes were substantially minimized in the Δ*ech*/Δ*frh*/Δ*vht* triple mutant, suggesting that both Frh and Vht inhibit methanol oxidation, which is needed to provide reducing equivalents for biosynthesis, when H_2 is present.

As previously reported, we were unable to obtain a mutant lacking only *vht*, suggesting that loss of this locus is lethal in otherwise wild-type strains (15). This conclusion was supported by the phenotype of the P_{tet}*vht* and P_{tet}*vht*/Δ*ech* mutants, which were incapable of growth on any medium when tetracycline is absent (*i.e.* under repressing conditions). However, as previously noted, when cells were grown on methanol it was possible to delete the *vht* operon if *frh* was deleted first. The Δ*frh*/Δ*vht* strains, including ones that also carried an *ech* deletion, had methanol growth phenotypes similar to that of the wild type. Thus, hydrogenases are not required for growth on methanol, although *vht*-deficient strains are inviable in the presence of an active Frh hydrogenase. In contrast, strains lacking *vht* alone or in combination with other mutations were unable to grow on either H_2/CO_2 or acetate media. A more graded response was observed when various *vht* mutants were grown on methanol/H_2/CO_2. Accordingly, on this substrate combination, the *vht* single mutant was inviable, while the *Δfrh*/*Δvht* double mutant grew very poorly and the *Δech*/*Δfrh*/*Δvht* strain had phenotypes that were nearly wild-type. Again,

these data are consistent with the idea that with certain mutant backgrounds Frh, Vht and Ech inhibit methanol oxidation in the presence of H_2.

Finally, mutants lacking only the *frh* operon grew on three out of four substrates tested, failing to grow only on H_2/CO_2 medium. When methanol was the sole substrate, the Δ*frh* mutant had an extended lag phase and a generation time approximately double that of the parental strain. However, during growth on either acetate or methanol/H_2/CO_2 the growth phenotypes of this strain were equivalent to the parental strain, suggesting Frh enhances growth on methanol, but is not required for growth on the two latter substrate combinations.

Methane and CO_2 production by hydrogenase deletion mutants. To probe the underlying mechanisms behind the growth phenotypes, we also examined production of methane and CO_2 by resting cell suspensions incubated with various substrates (Tables 2 & 3). The P_{tet}*vht* and P_{tet}*vht*/Δ*ech* mutants were not examined because they do not grow in any medium under non-inducing conditions. Similarly, we did not assay production of methane from acetate, because prior growth on acetate is required to induce the enzymes needed for this activity and most of the hydrogenase mutants are unable to grow under these conditions (20, 21).

Consistent with their lack of growth phenotypes, the Δ*fre* and Δ*vhx* single mutations did not affect the levels of methane produced from any substrate tested. Neither did these mutations affect the ratio of methane/CO_2 produced from methanol or from methanol/H_2. However, the Δ*vhx* mutation slowed the rate of methane production. The Δ*fre* mutation also slowed the rate of methane production, but only when combined with the Δ*frh* mutation.

As seen in previous studies, Δ*ech* mutants produced only minor amounts of methane from H_2/CO_2 (<2% relative to the parental strain), but produced wild-type levels from both methanol and methanol/H_2. During incubations with methanol, methane and CO_2 were produced in a 3:1 ratio, consistent with disproportionation of the substrate via the methylotrophic pathway (Fig 2). Cell suspensions incubated with methanol and H_2 produced only methane, showing that addition of hydrogen inhibits methanol oxidation. The rate of methane production by the Δ*ech* mutant was somewhat slower than wild-type using both methanol and methanol/H_2. This rate was further reduced when the *ech* deletion was combined with mutations removing the *frh* or *vht* operons. Accordingly, the Δ*ech*/Δ*frh* double mutant produced methane nearly 5 times slower than the wild-type strain. Interestingly, this mutant produced a small amount of CO_2 in addition to the wild-type level of methane, indicating a small amount of methanol was oxidized. When the *ech*, *frh,* and *vht* hydrogenases were deleted together, the quantity and stoichiometry of methane and CO_2 production was identical to that observed on methanol alone.

The Δ*frh* single mutant produced similar levels and ratios of methane and CO_2 relative to the parental strain with methanol or methanol/H_2. When H_2/CO_2 was the substrate, methane production was reduced *ca.* 10-fold, but, significantly, not abolished. Combining the Δ*frh* mutation with deletions of *vht* and *ech* reduced methane production from H_2/CO_2 to negligible levels. In contrast, minimal affects on methane and CO_2 production or stoichiometry were observed when methanol was the sole substrate. However, when combined with deletions of *vht* or *ech*, the Δ*frh* mutants produced significant levels of CO_2 when incubated with methanol/H_2, and

291 the triple Δ*ech*/Δ*frh*/Δ*vht* mutant produced similar levels to that seen in assays
292 incubated with methanol alone. Rates of methane production were substantially
293 slower than wild-type for all Δ*frh* mutants.

294 **Enzyme activity in hydrogenase mutants**. The hydrogenase activity for
295 selected deletion mutants was measured in the forward direction (H_2 oxidation) to
296 allow estimation of the contributions of each enzyme to overall activity (Table 4).

297 The hydrogenase activity of mutants lacking Fre or Vhx was not statistically
298 different from the parental strain. Moreover, hydrogenase activity of the
299 Δ*ech*/Δ*frh*/Δ*vht* mutant, which still encodes Fre and Vhx, was not statistically
300 different than the Δ*ech*/Δ*frh*/Δ*fre*/Δ*vht-vhx* mutant that lacks all five hydrogenase
301 operons. Thus, the *freAEGB* and *vhxGAC* operons do not, by themselves, produce
302 detectable levels of hydrogenase. Because Fre and Vhx are essentially inactive, the
303 hydrogenase levels in the Δ*frh*/Δ*vht* and Δ*ech*/Δ*frh* strains can be attributed solely
304 to Ech and Vht, respectively. Accordingly, Ech has the lowest activity of the three
305 hydrogenases, accounting for *ca.* 4% of total activity, and with Vht activity being *ca.*
306 6-fold higher. Consistent with this conclusion, deletion of *ech* did not significantly
307 affect hydrogenase activity, whereas the Δ*frh* strain had drastically diminished
308 activity as compared to the parental strain. Additionally, activity from the Δ*frh*
309 strain, which encodes both Vht and Ech, is roughly equivalent to the combined
310 activities of strains encoding only Vht or only Ech. Because strains expressing only
311 Frh hydrogenase are inviable, the activity of this hydrogenase cannot be directly
312 determined from a mutant strain. However, the relative contribution of Frh can be
313 estimated from the hydrogenase activities of other mutants. Thus, by subtracting

the activities of Vht and Ech from that of the parental strain, we estimate that roughly 75% of hydrogenase activity can be attributed to Frh.

Effect of hydrogenase deletions on mRNA abundance. Our estimate of the relative activities of the individual hydrogenases assumes that the expression levels for each hydrogenase are unaffected by deletion of the others. To explicitly examine this possibility, we determined the global mRNA abundance profiles for each mutant using RNA seq (Table S4 and Dataset S1). Importantly, the RNA used in this analysis was isolated from the same cultures that were assayed for hydrogenase activity.

As expected, the mRNA levels for the deleted genes in each mutant were significantly and substantially lower than the parental strain, providing an important validation that the correct strains were used in these assays. Moreover, no significant differences in mRNA abundance from the parent were observed for the remaining hydrogenases in any strain, showing that the expression of individual hydrogenase operons is not regulated by the presence/absence of other hydrogenase genes. Thus, the hydrogenase activities found in the various mutants accurately reflect the combined activities of each enzyme in all strains.

Large numbers of *M. barkeri* genes showed significant changes in mRNA abundance in the hydrogenase mutants, relative to the parental strain. Accordingly, 2.7% of all genes were differently regulated in strains with one or two deleted hydrogenases, whereas the Δ*ech*/Δ*frh*/Δ*vht* and Δ*ech*/Δ*frh*/Δ*fre*/Δ*vht-vhx* strains showed in 17.4% and 22.5% differently regulated genes, respectively (Dataset S1). Of these, most encode proteins with unknown functions or with annotated functions that do not appear to be related to energy conservation. One exception was the F420

dehydrogenase (*fpo*), whose mRNA abundance increased significantly in all strains lacking *frh* (Table S4). This result suggests that the cell has a mechanism to sense the redox state of F420, which is altered upon deletion of *frh*.

DISCUSSION

While fully consistent with the proposed functions of the *M. barkeri* hydrogenases, our phenotypic characterization of mutants lends new insight into the flexibility and interconnected nature of methanogenic metabolism. For example, reduction of CO_2 to CH_4 is expected to require three kinds of electron donors: Fd_{red}, $F420_{red}$, and reduced methanophenazine (1). Consistent with this idea, mutants lacking hydrogenases that reduce Fd (Ech), F420 (Frh) or methanophenazine (Vht) are unable to grow on H_2/CO_2. Thus, we were surprised to observe production of methane from H_2/CO_2 in cell suspensions of Δ*frh* mutants. Assuming this process involves the standard CO_2 reduction pathway, this would require an alternative source of $F420_{red}$ for reduction of methenyl- and methylene-tetrahydrosarcinapterin (Fig 2). Two alternative sources can be envisioned: first, Fpo could produce $F420_{red}$ using reduced methanophenazine as the electron donor via reverse electron transport driven by proton motive force; second, a soluble heterodisulfide reductase could produce $F420_{red}$ via electron bifurcation using CoM-S-S-CoB and Fd_{red} as substrates (as suggested in (22, 23)). In the former mechanism, reduced methanophenazine would be derived from H_2 using Vht; in the latter, Fd_{red} would be derived from H_2 via Ech. Interestingly, double mutants lacking Frh and either Ech or Vht produce much less methane than the Δ*frh* single mutant, thus both alternate

pathways may contribute to this phenotype. The inability of the Δ*frh* mutant to grow on H_2/CO_2 suggests that this alternate methane-producing pathway does not provide sufficient energy for growth, or that it fails to provide an essential biosynthetic precursor.

Similar metabolic flexibility is seen during methylotrophic methanogenesis, which can occur via H_2-dependent or -independent mechanisms (Figures 2, 3) (11, 12, 15, 16). We previously showed that a hydrogen cycling mechanism involving Frh and Vht is the preferred mode of electron transport in *M. barkeri*. Nevertheless, *M. barkeri* is also capable of methylotrophic growth in the absence of Frh and Vht (11, 15). Data reported here reveal that methylotrophic growth in *M. barkeri* is possible when all three hydrogenases are deleted. Thus, we have created an *M. barkeri* strain similar to *Methanosarcina acetivorans*, which has no detectable hydrogenase activity, but which grows well on methylotrophic substrates (7, 14). During methylotrophic growth in *M. acetivorans,* an electron transport chain comprised of Fpo and HdrDE is used to capture energy from $F420_{red}$ produced by the oxidative branch of the methanogenic pathway (Figures 2, 3). Our genetic analyses suggest that Fpo is also used to metabolize $F420_{red}$ in *M. barkeri* Δ*frh*/Δ*vht* mutants (11, 15). The oxidative branch of the methylotrophic pathway also produces Fd_{red}, which in *M. acetivorans* is oxidized by membrane-bound, ion-pumping Fd_{red}:methanophenazine oxidoreductase known as Rnf (24). However, because *M. barkeri* does not encode Rnf, this energy-conserving electron transport pathway in not available to the Ech mutants characterized here. Thus, an alternative Fd_{red}:heterodisulfide oxidoreductase system must exist to allow growth of these mutants on methanol. It

383 has been suggested that this alternate Fd_{red}:heterodisulfide oxidoreductase activity
384 is catalyzed by a cytoplasmic, electron-bifurcating heterodisulfide reductase
385 (HdrABC), similar to the electron-bifurcating heterodisulfide reductase of non-
386 cytochrome containing methanogens (Fig 3) (22). Biochemical data from a
387 homologous *M. acetivorans* enzyme supports this possibility (23).
388 Interestingly, the stoichiometry of methane and CO_2 produced from
389 methanol/H_2 in Δ*frh*/Δ*vht* and Δ*frh*/Δ*fre*/Δ*vht-vhx* mutants lends additional support
390 for an alternate Fd_{red}:heterodisulfide oxidoreductase. These strains, which encode
391 only Ech, might be expected to disproportionate methanol to CH_4 and CO_2 in a 3:1
392 ratio, as was seen in the strains lacking all three active hydrogenases. Instead, they
393 produced CH_4 and CO_2 at an approximate ratio of 10:1, suggesting that a substantial
394 portion of methanol was reduced directly to CH_4 using electrons obtained by H_2
395 oxidation. Because Ech is the sole remaining hydrogenase in these strains, electrons
396 from Fd_{red} must be involved in this process.
397 H_2 also inhibits oxidation of methanol when both substrates are present, via
398 a mechanism that is clearly mediated by hydrogenase activity. Accordingly, in the
399 presence of H_2, methanol is solely reduced to methane by cell suspensions of strains
400 that contain all three hydrogenases, while it is disproportionated to methane and
401 CO_2 in a 3:1 ratio when all three are absent. The hydrogenase-mediated inhibition of
402 methanol oxidation is graded, with Vht having the largest effect and Ech the least.
403 Similarly, Ech mutants are only able to grow on methanol/H_2 when supplemented
404 with acetate and pyruvate, which has been interpreted to mean they cannot produce
405 the reducing equivalents needed for biosynthesis by oxidizing methanol to CO_2 (16).

406 We showed here that this effect is alleviated by deletion of genes encoding Frh and
407 Vht, with the Δ*vht* mutation having a much larger effect. Because protein synthesis
408 was blocked by addition of puromycin in the cell suspension experiments, these
409 effects cannot have been mediated by changes in the concentration of enzymes in
410 the methanogenic pathways. Moreover, because inhibition requires the
411 hydrogenase enzymes to be present, it is likely that a product of the enzymatic
412 reaction mediates inhibition: namely the reduced enzyme cofactors. Thus, in the
413 presence of high H_2 partial pressures and the appropriate hydrogenase, we would
414 expect the levels of oxidized methanophenazine, $F420_{ox}$ and Fd_{ox} to be kept at very
415 low levels. Interestingly, the graded inhibition in response to loss of Vht, Frh and
416 Ech mimics the thermodynamics of the hydrogenase reactions, with
417 methanophenazine being the most energetically favorable electron acceptor and Fd
418 being the least. This suggests at least two possible mechanisms that might account
419 for the inhibition: *i)* allosteric inhibition or covalent inactivation of a key enzymatic
420 step in the oxidative branch of the pathway could be triggered by one or more
421 reduced cofactors, or *ii)* simple changes in the availability of $F420_{ox}$ and Fd_{ox}, which
422 are needed for three discrete steps in the oxidative branch of the methyloptrophic
423 pathway (Fig 2). Note that in the second mechanism, the major inhibitory effect of
424 Vht on methyl oxidation can only be explained if high levels of reduced
425 methanophenazine influence the levels of $F420_{ox}$, which could occur by changing the
426 equilibrium of the Fpo reaction (Fig 2, 3).
427 In addition to affecting flux through methanogenic pathways, the levels of
428 reduced or oxidized cofactors may be used as a sensory input to modulate gene

429 regulation. Transcriptional profiling of hydrogenase mutants showed that in all
430 strains lacking *frh*, the *fpo* operon was significantly up-regulated. Without Frh, Fpo
431 is solely responsible for the $F420_{red}$:methanophenazine oxidoreductase activity
432 required to transfer electrons from the oxidative to reductive portions of the
433 methylotrophic electron transport pathway. Elevated abundance of *fpo* mRNA in
434 Δ*frh* strains indicates that the cell has a mechanism to sense and respond to F420
435 redox imbalance. A previous study identified MreA as a global regulator in
436 *Methanosarcina* with the ability to bind and repress the *fpo* promoter region during
437 aceticlastic growth (25). This regulator was shown to affect gene expression based
438 on growth substrate, however the mechanism and sensory input are unknown.
439 Systems for gene regulation based on detected redox imbalance of F420 and other
440 electron carriers are a potential source for future studies.
441 The levels of hydrogenase activity for the three enzyme types have
442 significant ramifications for the hydrogen cycling model on energy conservation
443 (15). We have shown that Δ*vht* mutations are lethal when Frh is present, but not
444 when it is absent. Moreover, when *vht* expression is turned off using a regulated
445 promoter, cell lysis is concomitant with H_2 accumulation, implying that the inability
446 to recapture H_2 produced in the cytoplasm is responsible for the lethal phenotype.
447 With this in mind, it seems clear that the cytoplasmic activities of Frh must be
448 carefully balanced against the periplasmic activity of Vht. Interestingly, our data
449 show that Frh activity is ca. 3-fold higher than that of Vht. Thus, it appears that
450 ability of Frh to produce H_2 is much higher than the ability of Vht to take it up. We
451 recognize that our assays were not conducted with the native substrates (which are

not commercially available), therefore we approximated the *in vivo* activity of each enzyme based on available literature values in which a variety of natural and artificial cofactors were used (Table S5). These data suggest that the relative activities of Frh and Vht are more similar than our assay data suggest, with Frh activity ca. 1.5-fold higher than Vht. While this extrapolation must be interpreted with caution, it still suggests that Frh capacity is higher than that of Vht. In this regard, both Vht and Ech are coupled to ion-motive force; thus, activity in whole, metabolically active cells could be substantially different.

Finally, unlike Frh and Vht, Fre and Vhx are not able to provide sufficient levels of $F420_{red}$ and reduced methanophenazine, respectively, for growth via CO_2 reduction. Additionally, the Δ*ech*/Δ*frh*/Δ*vht* strain that only encoded for the Fre and Vhx hydrogenases had no detectable hydrogenase activity. This could be due to low expression of *fre* and *vhx* operons, absence of post-translational processing, mutations in structural or catalytic residues or some combination of these (7). Analysis of RNA sequencing data from wild type *M. barkeri* grown methylotrophically indicated the abundance mRNA for *fre* approximately 50-lower than *frh* (Dataset S1), similar to the relative abundance observed by Vaupel and Thauer (8). Additionally, the abundance of *vhx* transcripts was more than 200-fold lower than those of *vht*. We note that our enzymatic assays would have easily detected hydrogenase activity at levels 200-fold lower than we observed for the strains encoding only *vht*. Thus, poor gene expression cannot explain the lack of activity in strains expressing only Fre of Vhx. Hydrogenases require several maturation steps to become active enzymes, including processing by the maturation

proteases encoded by the *frhD* and *vhtD* genes. Thus, it remains possible that Fre and Vhx could encode active enzymes if FrhD and VhtD are *trans*-acting maturation proteases. Given that the mutants characterized here removed the entire *frh* and *vht* operons, our data do not address this possibility.

MATERIALS AND METHODS

Media and growth conditions

Methanosarcina strains were grown as single cells (26) at 37 °C in high salt (HS) broth medium (27) or on agar-solidified medium as described (28). Growth substrates provided were methanol (125 mM in broth medium and 50 mM in agar-solidified medium) or sodium acetate (120 mM) under a headspace of N_2:CO_2 (80:20 v/v) at 50 kPa over ambient pressure, H_2:CO_2 (80:20 v/v) at 300 kPa over ambient pressure, or a combination of methanol plus hydrogen. Cultures were supplemented as indicated with 0.1% yeast extract (YE), 0.1% casamino acids (CAA), 10 mM sodium acetate, 10 mM pyruvate or 100 mM pyruvate. Puromycin (CalBioChem, San Diego, CA) was added at 2 mg ml^{-1} for selection of the puromycin transacetylase (*pac*) gene (29). 8-Aza-2,6-diaminopurine (8-ADP) (Sigma, St Louis, MO) was added at 20 mg ml^{-1} for selection against the presence of *hpt* (29). Tetracycline (Tc) was added at 100 mg ml^{-1} to induce the tetracycline-regulated P*mcrB*(*tet*O1) promoter (19). Standard conditions were used for growth of *Escherichia coli* strains (30) DH5α/λ-*pir* (31) and DH10B (Stratagene, La Jolla, CA), which were used as hosts for plasmid constructions.

DNA methods and plasmid constructions

Standard methods were used for plasmid DNA isolation and manipulation in *E. coli* (32). Liposome mediated transformation was used for *Methanosarcina* as described (33). Genomic DNA isolation and DNA hybridization were as described (27, 28, 34). DNA sequences were determined from double-stranded templates by the W.M. Keck Center for comparative and functional genomics, University of Illinois. Plasmid constructions are described in Tables S1 and S2.

Strain construction in *M. barkeri*

The construction and genotype of all *Methanosarcina* strains is presented in Table S3. Hydrogenase encoding genes were deleted sequentially in a specific order (Figure S1) because certain hydrogenase deletion mutants are only viable when other hydrogenase genes are deleted first (15). To simplify isolation of strains that lack hydrogenase operons *vhxGAC* and *vhtGACD*, the genes between the two operons (*Mbar_A1842* and *Mbar_A1843*) were also deleted (Figure 1). All mutants were confirmed by either PCR or DNA hybridization (Figures S2-S5).

Determination of growth characteristics

For growth rate determinations, cultures were grown on methanol or methanol plus H_2/CO_2 (Δ*frh* and Δ*frh*/Δ*fre*) to mid-log phase (optical density at 600 nm [OD_{600}] *ca.* 0.5). Approximately 3% inoculum of the culture (or 10%, in case of acetate) was then transferred to fresh medium in at least four replicates and incubated at 37 °C. Growth was quantified by measuring OD_{600}. With the exception of samples grown on acetate, all OD_{600} were measured with a Spectronic 20 spectrophotometer (Thermo Fisher Scientific, Waltham, MA); those grown on acetate were measured with a Hewlett Packard 8453 spectrophotometer (Agilent,

Santa Clara, CA). Note that an OD of 1.0 on the Hewlett Packard 8453 is equivalent to an OD of ~0.2 on the Spectronic 20. Generation times were calculated during exponential growth phase and lag phase was defined as the time required to reach half-maximal OD_{600}.

Cell suspension experiments

Cells grown on methanol or methanol plus H_2/CO_2 (Δ*frh* and Δ*frh*/Δ*fre*) were collected in late exponential phase (OD_{600} = 0.6-0.7) by centrifugation at 5,000 x g for 15 minutes at 4 °C. The cells were washed once with anaerobic HS PIPES buffer (50 mM PIPES at pH 6.8, 400 mM NaCl, 13 mM KCl, 54 mM $MgCl_2$, 2 mM $CaCl_2$, 2.8 mM cysteine, 0.4 mM Na_2S) and resuspended in the same buffer to a final concentration of 10^9 cells/ml. Cells were counted visually using the Petroff-Hausser counting chamber (Hausser Scientific, PA). All assay mixtures contained 2 ml of the suspension and were conducted under strictly anaerobic conditions in 25 ml Balch tubes sealed with butyl rubber stoppers using 250 mM methanol as the methanogenic substrate under a headspace of N_2, H_2, or H_2/CO_2 (80/20%) at 250 kPa over the ambient pressure, as indicated. Puromycin (20 μg/ml) was added to prevent protein synthesis. Cells were held on ice until initiation of assay by transfer to 37 °C. For rate determination, gas phase samples were withdrawn at various time points and assayed for CH_4 by gas chromatography at 225 °C in a Hewlett Packard gas chromatograph (5890 Series II) equipped with a flame ionization detector. The column used was stainless steel filled with 80/120 Carbopack™ B/3% SP™-1500 (Supelco, Bellefonte, PA) with helium as the carrier gas. For total CH_4 and CO_2 production, assays were incubated at 37 °C for 36 hours prior to withdrawal of gas

phase samples for analysis by GC at 225 °C in a Hewlett Packard gas chromatograph (5890 Series II) equipped with a thermal conductivity detector. A stainless steel 60/80 Carboxen-1000 column (Supelco, Bellefonte, PA) with helium as the carrier gas was used. Total cell protein was determined using the Bradford method (35) after 1 ml of the cells was lysed by resuspension in dd$H_2$0 with 1 mg/ml RNase and DNase.

Hydrogenase assays

Strains were grown at 37 °C in HS medium supplemented with 125 mM methanol and cells were harvested from 10 ml mid-exponential phase culture at 1228 x *g* for 15 min in an IEC MediSpin (Needham Heights, MA) benchtop centrifuge. Preparation of cell extract was performed in an anaerobic chamber under an atmosphere of H_2/N_2 (4/96%). Cells were washed once in 10 ml HS-MOPS [2 mM dithiothreitol (DTT), 400 mM NaCl, 13 mM KCl, 54 mM $MgCl_2$, 2 mM $CaCl_2$, 50 mM MOPS, pH 7.0] and lysed in 1 ml lysis buffer (2 mM DTT, 0.5% *n*-dodecyl β-D-maltoside, *ca.* 50 Kunitz units bovine pancreas deoxyribonuclease I, 50 mM MOPS, pH 7.0) on ice for 30 min. Enzyme-containing supernatant was separated from cell debris by centrifugation at 13600 x *g* for 2.5 min (Fisher Scientific Micro Centrifuge Model 235C, Waltham, MA). Protein concentration was measured via the Bradford method (35).

Assays were performed anaerobically in 1.7 ml quartz cuvettes sealed with rubber stoppers. A total reaction volume of 1 ml was used, and included cell extract mixed with 50 mM MOPS buffer (pH 7.0) containing 2 mM DTT and 2 mM benzyl viologen (BV). The cuvette headspace was pressurized to 30 kPa with 100% H_2 after

being flushed for 2 min. Cuvettes with reaction mixture were pre-warmed to 30 °C before the reaction was initiated by the addition of BV. Hydrogenase activity was determined by quantifying the change in absorbance of BV at 578 nm (extinction coefficient, 8.65 cm^{-1} mM^{-1}) with a Cary 50 UV-Vis Spectrophotometer (Agilent, Santa Clara, CA). One unit (U) of hydrogenase activity was defined as the oxidation of 1 µmol H_2 per minute, based on the fact that 2 µmol BV are reduced for each H_2 oxidized. A minimum of three independent measurements from biological replicates was performed for each strain.

RNA sequencing

Immediately prior to cell harvest for hydrogenase assays, 2.5 ml of the same culture was harvested for total RNA isolation. An equal volume of TRIzol reagent (Ambion, Carlsbad, CA) was added to the culture to lyse cells and samples were incubated at room temperature for 5 min. RNA was then isolated with a Direct-zol RNA MiniPrep kit from Zymo Research (Irvine, CA) according to the manufacturer's directions. RNA samples were stored at -80 °C.

To increase coverage of mRNA during sequencing, rRNA was removed from samples via subtractive hybridization. The method of Stewart et al. (36) was utilized with the following modifications. Templates for 16S and 23S rRNA probes were generated by PCR from strain WWM85 with primers 16SFor, T716SRev, 23SFor, and T723SRev. *In vitro* transcription with the MEGAscript High Yield Transcription kit (Ambion) was used for the production of biotinylated antisense rRNA probes from 400 ng of the purified PCR products in separate reactions. After removal of template with DNAseI, probes were purified with the Zymo Research RNA Clean &

590 Concentrator kit. Hybridization reactions (30 µl) for each sample contained the
591 following: 20% formamide, 1X SSC buffer, 20 U SUPERase inhibitor, 2 µg total RNA,
592 4 µg 16S probe, and 4 µg 23S probe. Reactions were denatured at 70 °C for 10 min,
593 ramped down to 25 °C (-0.1 °C sec^{-1}), and incubated at room temperature for 10 min.
594 rRNA hybridized to biotinylated probe was removed via streptavidin-coated
595 magnetic beads (New England Biolabs, Ipswich, MA). Beads (500 µl per sample)
596 were washed twice with 500 µl 1X SSC buffer prior to the addition of hybridized
597 RNA sample diluted to 250 µl in 1X SSC buffer with 20% formamide. Samples were
598 incubated for 1 hour at room temperature with gentle shaking before separation of
599 beads on a magnetic rack. The supernatant was removed, beads were washed with
600 250 µl 1X SSC, and supernatant and wash were pooled and cleaned with the Zymo
601 Research RNA Clean & Concentrator kit.
602 Preparation and sequencing of RNAseq libraries was performed at the Roy J.
603 Carver Biotechnology Center at the University of Illinois at Urbana-Champaign.
604 Libraries were made with the TruSeq Stranded mRNA Sample Prep kit, sequenced
605 with a HiSeq 2000 using the TruSeq SBS v3 kit, and processed with Casava 1.8.2, all
606 per the manufacturer's directions (Illumina, San Diego, CA). All sequencing data was
607 further processed and analyzed as previously described (37) with CLC Genomics
608 Workbench 7 (Qiagen). Within this program, the Empirical analysis of Differential
609 Gene Expression (EDGE) tool was used for statistical analysis (38). Differently
610 regulated genes were considered significant when up- or down-regulated at least 3-
611 fold with a p-value ≤ 0.05. Three biological replicates were sequenced and analyzed

612 for each strain. Raw and processed data have been deposited in the Gene Expression
613 Omnibus (GEO) under the accession number GSE98441.
614

615 **ACKNOWLEDGEMENTS**

616 The authors acknowledge the Division of Chemical Sciences, Geosciences, and
617 Biosciences, Office of Basic Energy Sciences of the U.S. Department of Energy
618 through Grant DE-FG02-02ER15296 for funding of this work.

619 **REFERENCES**

620 1. Thauer RK, Hedderich R, Fischer R. 1993. Reactions and Enzymes Involved in
621 Methanogenesis from CO_2 and H_2, p 209-252. *In* Ferry JG (ed),
622 Methanogenesis: Ecology, Physiology, Biochemistry & Genetics. Chapman &
623 Hall, New York, NY.
624 2. Vignais PM, Billoud B, Meyer J. 2001. Classification and phylogeny of
625 hydrogenases. FEMS Microbiol Rev 25:455-501.
626 3. Peters JW, Schut GJ, Boyd ES, Mulder DW, Shepard EM, Broderick JB, King PW,
627 Adams MWW. 2015. [FeFe]- and [NiFe]-hydrogenase diversity, mechanism,
628 and maturation. Biochim Biophys Acta 1853:1350-1369.
629 4. Thauer RK, Kaster A-K, Goenrich M, Schick M, Hiromoto T, Shima S. 2010.
630 Hydrogenases from methanogenic archaea, nickel, a novel cofactor, and H_2
631 storage. Annu Rev Biochem 79:507-536.
632 5. Thauer RK, Kaster A-K, Seedorf H, Buckel W, Hedderich R. 2008.
633 Methanogenic archaea: ecologically relevant differences in energy
634 conservation. Nat Rev Microbiol 6:579-591.
635 6. Lie TJ, Costa KC, Lupa B, Korpole S, Whitman WB, Leigh JA. 2012. Essential
636 anaplerotic role for the energy-converting hydrogenase Eha in
637 hydrogenotrophic methanogenesis. Proc Natl Acad Sci U S A 109:15473-
638 15478.
639 7. Guss AM, Kulkarni G, Metcalf WW. 2009. Differences in hydrogenase gene
640 expression between *Methanosarcina acetivorans* and *Methanosarcina barkeri.*
641 J Bacteriol 191:2826-2833.

642 8. Vaupel M, Thauer RK. 1998. Two F_{420}-reducing hydrogenases in
643 *Methanosarcina barkeri*. Arch Microbiol 169:201-205.
644 9. Fiebig K, Friedrich B. 1989. Purification of the F_{420}-reducing hydrogenase
645 from *Methanosarcina barkeri* (strain Fusaro). Eur J Biochem 184:79-88.
646 10. Michel R, Massanz C, Kostka S, Richter M, Fiebig K. 1995. Biochemical
647 characterization of the 8-hydroxy-5-deazaflavin-reactive hydrogenase from
648 *Methanosarcina barkeri* Fusaro. Eur J Biochem 233:727-735.
649 11. Kulkarni G, Kridelbaugh DM, Guss AM, Metcalf WW. 2009. Hydrogen is a
650 preferred intermediate in the energy-conserving electron transport chain of
651 *Methanosarcina barkeri*. Proc Natl Acad Sci U S A 106:15915-15920.
652 12. Meuer J, Bartoschek S, Koch J, Künkel A, Hedderich R. 1999. Purification and
653 catalytic properties of Ech hydrogenase from *Methanosarcina barkeri*. Eur J
654 Biochem 265:325-335.
655 13. Liu Y, Whitman WB. 2008. Metabolic, Phylogenetic, and Ecological Diversity
656 of the Methanogenic Archaea. Ann N Y Acad Sci 1125:171-189.
657 14. Guss AM, Mukhopadhyay B, Zhang JK, Metcalf WW. 2005. Genetic analysis of
658 *mch* mutants in two *Methanosarcina* species demonstrates multiple roles for
659 the methanopterin-dependent C-1 oxidation/reduction pathway and
660 differences in H_2 metabolism between closely related species. Mol Microbiol
661 55:1671-1680.
662 15. Kulkarni G, Mand TD, Metcalf WW. 2018. Energy conservation via hydrogen
663 cycling in the methanogenic archaeon *Methanosarcina barkeri*. bioRxiv
664 https://doi.org/.

16. Meuer J, Kuettner HC, Zhang JK, Hedderich R, Metcalf WW. 2002. Genetic analysis of the archaeon *Methanosarcina barkeri* Fusaro reveals a central role for Ech hydrogenase and ferredoxin in methanogenesis and carbon fixation. Proc Natl Acad Sci U S A 99:5632-5637.

17. Deppenmeier U. 2004. The membrane-bound electron transport system of *Methanosarcina* species. J Bioenerg Biomembr 36:55-64.

18. Welte C, Deppenmeier U. 2014. Bioenergetics and anaerobic respiratory chains of aceticlastic methanogens. Biochim Biophys Acta 1837:1130-1147.

19. Guss AM, Rother M, Zhang JK, Kulkarni G, Metcalf WW. 2008. New methods for tightly regulated gene expression and highly efficient chromosomal integration of cloned genes for *Methanosarcina* species. Archaea 2:193-203.

20. Krzycki JA, Wolkin RH, Zeikus JG. 1982. Comparison of unitrophic and mixotrophic substrate metabolism by acetate-adapted strain of *Methanosarcina barkeri*. J Bacteriol 149:247-254.

21. Jablonski PE, DiMarco AA, Bobik TA, Cabell MC, Ferry JG. 1990. Protein content and enzyme activities in methanol- and acetate-grown *Methanosarcina thermophila*. J Bacteriol 172:1271-1275.

22. Buan NR, Metcalf WW. 2010. Methanogenesis by M*ethanosarcina acetivorans* involves two structurally and functionally distinct classes of heterodisulfide reductase. Mol Microbiol 75:843-853.

23. Yan Z, Wang M, Ferry JG. 2017. A Ferredoxin- and $F_{420}H_2$-Dependent, Electron-Bifurcating, Heterodisulfide Reductase with Homologs in the Domains Bacteria and Archaea. mBio 8: e02285-16.

688 24. Li Q, Li L, Rejtar T, Lessner DJ, Karger BL, Ferry JG. 2006. Electron transport
689 in the pathway of acetate conversion to methane in the marine archaeon
690 *Methanosarcina acetivorans*. J Bacteriol 188:702-710.
691 25. Reichlen MJ, Vepachedu VR, Murakami KS, Ferry JG. 2012. MreA functions in
692 the global regulation of methanogenic pathways in *Methanosarcina*
693 *acetivorans*. mBio 3:e00189-12.
694 26. Sowers KR, Boone JE, Gunsalus RP. 1993. Disaggregation of *Methanosarcina*
695 spp. and Growth as Single Cells at Elevated Osmolarity. Appl Environ
696 Microbiol 59:3832-3839.
697 27. Metcalf WW, Zhang JK, Shi X, Wolfe RS. 1996. Molecular, genetic, and
698 biochemical characterization of the *serC* gene of *Methanosarcina barkeri*
699 Fusaro. J Bacteriol 178:5797-5802.
700 28. Boccazzi P, Zhang JK, Metcalf WW. 2000. Generation of dominant selectable
701 markers for resistance to pseudomonic acid by cloning and mutagenesis of
702 the *ileS* gene from the archaeon *Methanosarcina barkeri* Fusaro. J Bacteriol
703 182:2611-2618.
704 29. Pritchett MA, Zhang JK, Metcalf WW. 2004. Development of a markerless
705 genetic exchange method for *Methanosarcina acetivorans* C2A and its use in
706 construction of new genetic tools for methanogenic archaea. Appl Environ
707 Microbiol 70:1425-1433.
708 30. Wanner BL. 1986. Novel regulatory mutants of the phosphate regulon in
709 *Escherichia coli* K-12. J Mol Biol 191:39-58.

31. Miller VL, Mekalanos JJ. 1988. A novel suicide vector and its use in construction of insertion mutations: osmoregulation of outer membrane proteins and virulence determinants in *Vibrio cholerae* requires *toxR*. J Bacteriol 170:2575-2583.

32. Ausubel FM, Brent R, Kingston RE, Moore DD, Seidman JG, Smith JA, Struhl K. 1992. Current Protocols in Molecular Biology. Wiley & Sons, New York.

33. Metcalf WW, Zhang JK, Apolinario E, Sowers KR, Wolfe RS. 1997. A genetic system for Archaea of the genus *Methanosarcina*: liposome-mediated transformation and construction of shuttle vectors. Proc Natl Acad Sci U S A 94:2626-2631.

34. Zhang JK, White AK, Kuettner HC, Boccazzi P, Metcalf WW. 2002. Directed mutagenesis and plasmid-based complementation in the methanogenic archaeon *Methanosarcina acetivorans* C2A demonstrated by genetic analysis of proline biosynthesis. J Bacteriol 184:1449-1454.

35. Bradford MM. 1976. A rapid and sensitive method for the quantitation of microgram quantities of protein utilizing the principle of protein-dye binding. Anal Biochem 72:248-254.

36. Stewart FJ, Ottesen EA, DeLong EF. 2010. Development and quantitative analyses of a universal rRNA-subtraction protocol for microbial metatranscriptomics. ISME J 4:896-907.

37. Fu H, Metcalf WW. 2015. Genetic basis for metabolism of methylated sulfur compounds in *Methanosarcina* species. J Bacteriol 197:1515-1524.

732 38. Robinson MD, Smyth GK. 2008. Small-sample estimation of negative binomial
733 dispersion, with applications to SAGE data. Biostatistics 9:321-332.

734

735

FIGURE LEGENDS

Fig 1. Hydrogenase operons of *Methanosarcina barkeri*. Three distinct types of hydrogenase are encoded by *M. barkeri*. Two potential methanophenazine-dependent hydrogenases are encoded by the adjacent *vhtGACD* and *vhxGAC* operons, while two potential F420-dependent hydrogenases are encoded by the unlinked *frhADGB* and *freAEGB* operons. The energy-converting, ferredoxin-dependent hydrogenase is encoded by the *echABCDEF* operon. Locus Tags are shown below each gene, in some cases the "Mbar_" prefix was omitted (shown by an asterisk) due to space constraints.

Fig 2. Four methanogenic pathways of *Methanosarcina*. Each pathway shares a common step in the reduction of methyl-CoM to methane; however, they differ in the route used to form methyl-CoM and in the source of electrons used for its reduction to methane. The CO_2 reduction pathway (red arrows) involves reduction of CO_2 to methane using electrons derived from the oxidation of H_2, while the methylotrophic pathway (light blue arrows) involves disproportionation of C-1 substrates to methane and CO_2. These two pathways share many steps, with overall metabolic flux in opposite directions (shown by red/light blue shaded arrows). In the aceticlastic pathway (green arrows), acetate is split into a methyl group and an enzyme-bound carbonyl moiety (shown in brackets) by the enzyme acetyl-CoA decarbonylase/synthase (ACDS). The latter is oxidized to CO_2, producing reduced ferredoxin that provides electrons for reduction of methyl group to methane. Lastly, in the methyl reduction pathway (dark blue arrows) C-1 compounds are reduced to

CH_4 using electrons derived from H_2 oxidation. Dashed lines depict diffusion of H_2, which occurs during the transfer of electrons between oxidative and reductive portions of methylotrophic and aceticlastic pathways. The steps catalyzed by Frh, Vht, Ech hydrogenases are indicated. Note that in wild-type *M. barkeri* hydrogenases are involved in all four pathways. Abbreviations used are: Hdr, heterodisulfide reductase; MF, methanofuran; H_4SPT, tetrahydrosarcinapterin; CoM, coenzyme M; CoB, coenzyme B; CoM-S-S-CoB, heterodisulfide of CoM and CoB; Fd_{ox}/Fd_{red}, oxidized and reduced ferredoxin; $F420_{ox}/F420_{red}$, oxidized and reduced cofactor F420; MP_{ox}/MP_{red}, oxidized and reduced methanophenazine.

Fig 3. The branched electron transport systems of *Methanosarcina barkeri* and *Methanosarcina acetivorans.* During methylotrophic methanogenesis, *M. barkeri* can utilize H_2-dependent or H_2-independent electron transport systems. The H_2-dependent pathway involves the use of hydrogenases Frh, Ech, and Vht in a H_2 cycling mechanism to transfer electrons from $F420_{red}$ or Fd_{red} to methanophenazine (MP). *M. acetivorans* does not utilize hydrogenases, and is therefore incapable of H_2 cycling. Both organisms can conserve energy via a H_2-independent pathway, wherein electrons are transferred from $F420_{red}$ to MP by way of the F420 dehydrogenase (Fpo). Additionally, the electron transport system in *M. acetivorans* includes the Na^+-translocating Rnf enzyme complex that serves as a Fd:MP oxidoreductase. Both membrane-bound electron transport systems converge at the reduction of the CoM-S-S-CoB heterodisulfide with electrons from reduced MP_{red} via the cytochrome-containing HdrDE enzyme. Protons (or Na^+ in the case of Rnf) are

translocated across the cell membrane in both systems, thereby conserving energy in the form of an ion motive force. An additional heterodisulfide reductase, HdrA1B1C1, has been proposed to function in the energy conservation pathways for both organisms. This electron bifurcating enzyme potentially reduces both the CoM-S-S-CoB heterodisulfide and F420 with electrons from Fd_{red} at a stoichiometric ratio of 2 Fd_{red} oxidized for the reduction of 1 CoM-S-S-CoB to CoM-SH/CoB-SH and reduction of 1 $F420_{ox}$ to $F420_{red}$. Abbreviations used are: Fd_{ox}/Fd_{red}, oxidized and reduced ferredoxin; MP/MPH_2, oxidized and reduced methanophenazine; $F420_{ox}$/$F420_{red}$, oxidized and reduced F420; CoM, coenzyme M; CoB, coenzyme B; CoM-S-S-CoB, heterodisulfide of CoM and CoB; FeS, iron-sulfur cluster; FAD, flavin adenine dinucleotide; FMN, flavin mononucleotide; NiFe, nickel-iron active site of hydrogenases; $cytb_1$/$cytb_2$/cyt c, cytochromes.

TABLES

Table 1. Growth of *M. barkeri* mutant strains on various methanogenic substrates.

	H_2/CO_2			Methanol			Methanol/H_2/CO_2			Acetate		
Genotype	Gen. (h)[d]	Max. OD[e]	Lag (h)	Gen. (h)[d]	Max. OD[e]	Lag (h)	Gen. (h)[d]	Max. OD[e]	Lag (h)	Gen. (h)[d]	Max. OD[f]	Lag (h)
Δ*hpt*[a]	10.4 ± 0.7	0.42 ± 0.04	49 ± 11	8.9 ± 0.3	0.85 ± 0.05	36 ± 1	6.2 ± 0.5	0.77 ± 0.03	33 ± 1	43.6 ± 2.2	1.65 ± 0.04	195 ± 11
Δ*fre*	10.3 ± 0.6	0.35 ± 0.03	59 ± 1	8.8 ± 0.4	0.78 ± 0.04	37 ± 1	7.0 ± 0.4	0.68 ± 0.01	38 ± 4	38.6 ± 2.3	1.68 ± 0.05	200 ± 13
Δ*vhx*	10.7 ± 0.5	0.45 ± 0.02	60 ± 3	8.5 ± 0.2	0.78 ± 0.08	36 ± 2	7.5 ± 0.5	0.69 ± 0.04	51 ± 3	47.2 ±3.8	1.70 ± 0.08	181 ± 22
Δ*ech*	NG	NA	NA	12.2 ± 0.9	0.69 ± 0.05	46 ± 1	NG	NA	NA	NG	NA	NA
Δ*ech*/Δ*frh*	NG	NA	NA	12.1 ± 0.7	0.80 ± 0.05	54 ± 2	13 ± 2	0.54 ± 0.03	248 ± 17	NG	NA	NA
Δ*ech*/Δ*frh*/Δ*vht*	NG	NA	NA	10.8 ± 0.2	0.71 ± 0.06	48 ± 3	9.0 ± 0.4	0.61 ± 0.02	48 ± 2	NG	NA	NA
Δ*ech*/Δ*frh*/Δ*fre*/Δ*vht-vhx*[c]	NG	NA	NA	12.1 ± 0.2	0.84 ± 0.06	54 ± 2	9.3 ± 0.1	0.68 ± 0.03	45 ± 1	NG	NA	NA
P_{tet}*vht*[b]	NG	NA	NA	NG	NA	NA	NG	NA	NA	NG	NA	NA
P_{tet}*vht*/Δ*ech*[b]	NG	NA	NA	NG	NA	NA	NG	NA	NA	NG	NA	NA
Δ*frh*/Δ*vht*	NG	NA	NA	11.7 ± 0.7	0.89 ± 0.01	54 ± 2	35 ± 3	0.33 ± 0.03	151 ± 4	NG	NA	NA
Δ*frh*/Δ*fre*/Δ*vht-vhx*[c]	NG	NA	NA	12.3 ± 0.6	0.84 ± 0.07	58 ± 2	29 ± 2	0.43 ± 0.03	116 ± 3	NG	NA	NA
Δ*frh*	NG	NA	NA	19.5 ± 1.0	0.69 ± 0.05	122 ± 6	7.4 ± 0.6	0.64 ± 0.14	45 ± 3	38.2 ± 1.7	1.71 ± 0.03	219 ± 11
Δ*frh*/Δ*fre*	NG	NA	NA	16.5 ± 0.8	0.80 ± 0.00	89 ± 2	7.7 ± 0.2	0.74 ± 0.01	48 ± 1	39.6 ± 2.9	1.63 ± 0.07	170 ± 13

[a] *M. barkeri* Fusaro parental strain; [b] Growth in the absence of tetracycline; [c] *Mbar_A1842* and *Mbar_1843* also deleted; [d] Generation (doubling) time; [e] Optical Density was measured on a Spectronic 20 spectrophotometer at 600 nm; [f] Optical Density was measured on a Hewlett Packard 8453 spectrophotometer at 600 nm. Note that an OD of 1.0 on the Hewlett Packard 8453 is equivalent to an OD of ~0.2 on the Spectronic 20. NG, no growth for at least 6 months of incubation; NA, not applicable.

803 **Table 2. Production of CH_4 and CO_2 from resting cell suspensions of *M. barkeri* mutant strains.**

	H_2/CO_2		Methanol			Methanol/H_2		
Genotype	CH_4[a]	CO_2[a]	CH_4[a]	CO_2[a]	CH_4: CO_2	CH_4[a]	CO_2[a]	CH_4: CO_2
Δ*hpt*[b]	307 ± 24	NA	339 ± 6	118 ± 2	2.9:1	458 ± 6	< 1	
Δ*fre*	316 ± 16	NA	339 ± 7	117 ± 2	2.9:1	442 ± 24	< 1	
Δ*vhx*	328 ± 21	NA	329 ± 7	113 ± 3	2.9:1	453 ± 6	< 1	
Δ*ech*	5 ± 1	NA	331 ± 6	109 ± 2	3.0:1	460 ± 12	< 1	
Δ*ech*/Δ*frh*	3 ± 0	NA	328 ± 7	107 ± 2	3.1:1	440 ± 14	4 ± 1	110:1
Δ*ech*/Δ*frh*/Δ*vht*	1 ± 0	NA	315 ± 5	93 ± 1	3.4:1	313 ± 5	92 ± 2	3.4:1
Δ*ech*/Δ*frh*/Δ*fre*/Δ*vht-vhx*[c]	1 ± 0	NA	314 ± 2	94 ± 1	3.3:1	315 ± 8	93 ± 3	3.4:1
Δ*frh*	34 ± 1	NA	310 ± 8	96 ± 2	3.2:1	442 ± 4	< 1	
Δ*frh*/Δ*fre*	10 ± 2	NA	298 ± 13	98 ± 4	3.0:1	436 ± 8	< 1	
Δ*frh*/Δ*vht*	6 ± 1	NA	311 ± 5	92 ± 1	3.4:1	225 ± 16	20 ± 1	11:1
Δ*frh*/Δ*fre*/Δ*vht-vhx*[c]	5 ± 0	NA	309 ± 6	92 ± 2	3.4:1	300 ± 8	19 ± 1	16:1

804 [a] µmol product observed; [b] *M. barkeri* Fusaro parental strain; [c] *Mbar_A1842* and *Mbar_1843* also deleted; NA, not applicable as

805 produced CO_2 could not be differentiated from CO_2 that was added to the headspace. When relevant, ratio of CH_4:CO_2 is shown.

806 CH_4 and CO_2 quantities were below 4 ± 1 µmol for each strain when measured in cell suspensions without substrate.

807 **Table 3. Rate of CH_4 production[a] from resting cell suspensions of *M. barkeri***

808 **mutant strains.**

Genotype	Methanol	Methanol & H_2
Δ*hpt*[b]	86 ± 7	132 ± 18
Δ*fre*	84 ± 1	123 ± 16
Δ*vhx*	71 ± 2	74 ± 12
Δ*ech*	57 ± 5	122 ± 7
Δ*ech*/Δ*frh*	20 ± 1	27 ± 3
Δ*ech*/Δ*frh*/Δ*vht*	31 ± 2	30 ± 3
Δ*ech*/Δ*frh*/Δ*fre*/Δ*vht-vhx*[c]	19 ± 2	19 ± 2
Δ*frh*	23 ± 1	136 ± 9
Δ*frh*/Δ*fre*	14 ± 1	87 ± 3
Δ*frh*/Δ*vht*	38 ± 8	36 ± 4
Δ*frh*/Δ*fre*/Δ*vht-vhx*[c]	32 ± 10	34 ± 13

809 [a] nmol methane produced min^{-1} mg^{-1}; [b] *M. barkeri* Fusaro parental strain; [c]

810 *Mbar_A1842* and *Mbar_1843* also deleted.

811

812

Table 4. Hydrogenase activity of *M. barkeri* mutant strains.

Genotype	Specific Activity[a]
Δ*hpt*[b]	11.10 ± 4.29
Δ*fre*	9.18 ± 4.38
Δ*vhx*	8.51 ± 3.93
Δ*ech*/Δ*frh*/Δ*vht*	**0.01 ± 0.00[d]**
Δ*ech*/Δ*frh*/Δ*fre*/Δ*vht-vhx*[c]	**0.02 ± 0.00**
Δ*ech*	17.13 ± 4.90
Δ*frh*/Δ*vht*	**0.42 ± 0.09**
Δ*ech*/Δ*frh*	**2.60 ± 1.36**
Δ*frh*	**3.12 ± 1.89**

[a] μmol H_2 oxidized min^{-1} mg^{-1}; [b] *M. barkeri* Fusaro parental strain; [c] *Mbar_A1842* and *Mbar_A1843* also deleted; [d] values that are significantly different (p-value < 0.01) than the Δ*hpt* parental strain are indicated in bold.

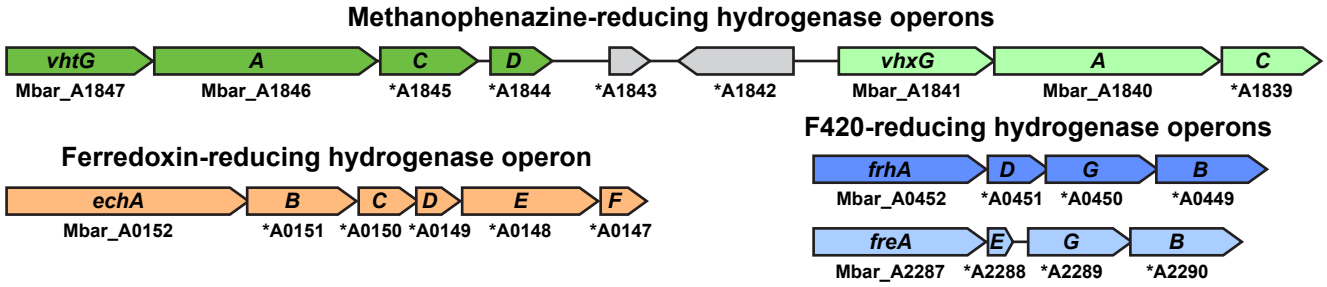

Fig 1. Hydrogenase operons of *Methanosarcina barkeri*. Three distinct types of hydrogenase are encoded by *M. barkeri*. Two potential methanophenazine-dependent hydrogenases are encoded by the adjacent *vhtGACD* and *vhxGAC* operons, while two potential F420-dependent hydrogenases are encoded by the unlinked *frhADGB* and *freAEGB* operons. The energy-converting, ferredoxin-dependent hydrogenase is encoded by the *echABCDEF* operon. Locus Tags are shown below each gene, in some cases the "Mbar_" prefix was omitted (shown by an asterisk) due to space constraints.

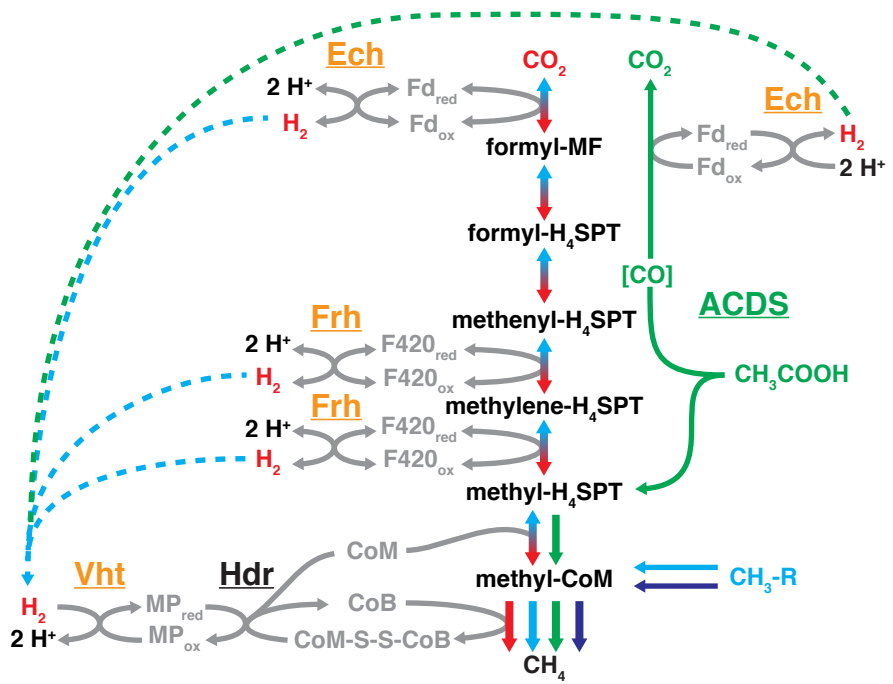

Fig 2. Four methanogenic pathways of *Methanosarcina*. Each pathway shares a common step in the reduction of methyl-CoM to methane; however, they differ in the route used to form methyl-CoM and in the source of electrons used for its reduction to methane. The CO_2 reduction pathway (red arrows) involves reduction of CO_2 to methane using electrons derived from the oxidation of H_2, while the methylotrophic pathway (light blue arrows) involves disproportionation of C-1 substrates to methane and CO_2. These two pathways share many steps, with overall metabolic flux in opposite directions (shown by red/light blue shaded arrows). In the aceticlastic pathway (green arrows), acetate is split into a methyl group and an enzyme-bound carbonyl moiety (shown in brackets) by the enzyme acetyl-CoA decarbonylase/synthase (ACDS). The latter is oxidized to CO_2, producing reduced ferredoxin that provides electrons for reduction of methyl group to methane. Lastly, in the methyl reduction pathway (dark blue arrows) C-1 compounds are reduced to CH_4 using electrons derived from H_2 oxidation. Dashed lines depict diffusion of H_2, which occurs during the transfer of electrons between oxidative and reductive portions of methylotrophic and aceticlastic pathways. The steps catalyzed by Frh, Vht, Ech hydrogenases are indicated. Note that in wild-type M. barkeri hydrogenases are involved in all four pathways. Abbreviations used are: Hdr, heterodisulfide reductase; MF, methanofuran; H_4SPT, tetrahydrosarcinapterin; CoM, coenzyme M; CoB, coenzyme B; CoM-S-S-CoB, heterodisulfide of CoM and CoB; Fd_{ox}/Fd_{red}, oxidized and reduced ferredoxin; $F420_{ox}/F420_{red}$, oxidized and reduced cofactor F420; MP_{ox}/MP_{red}, oxidized and reduced methanophenazine.

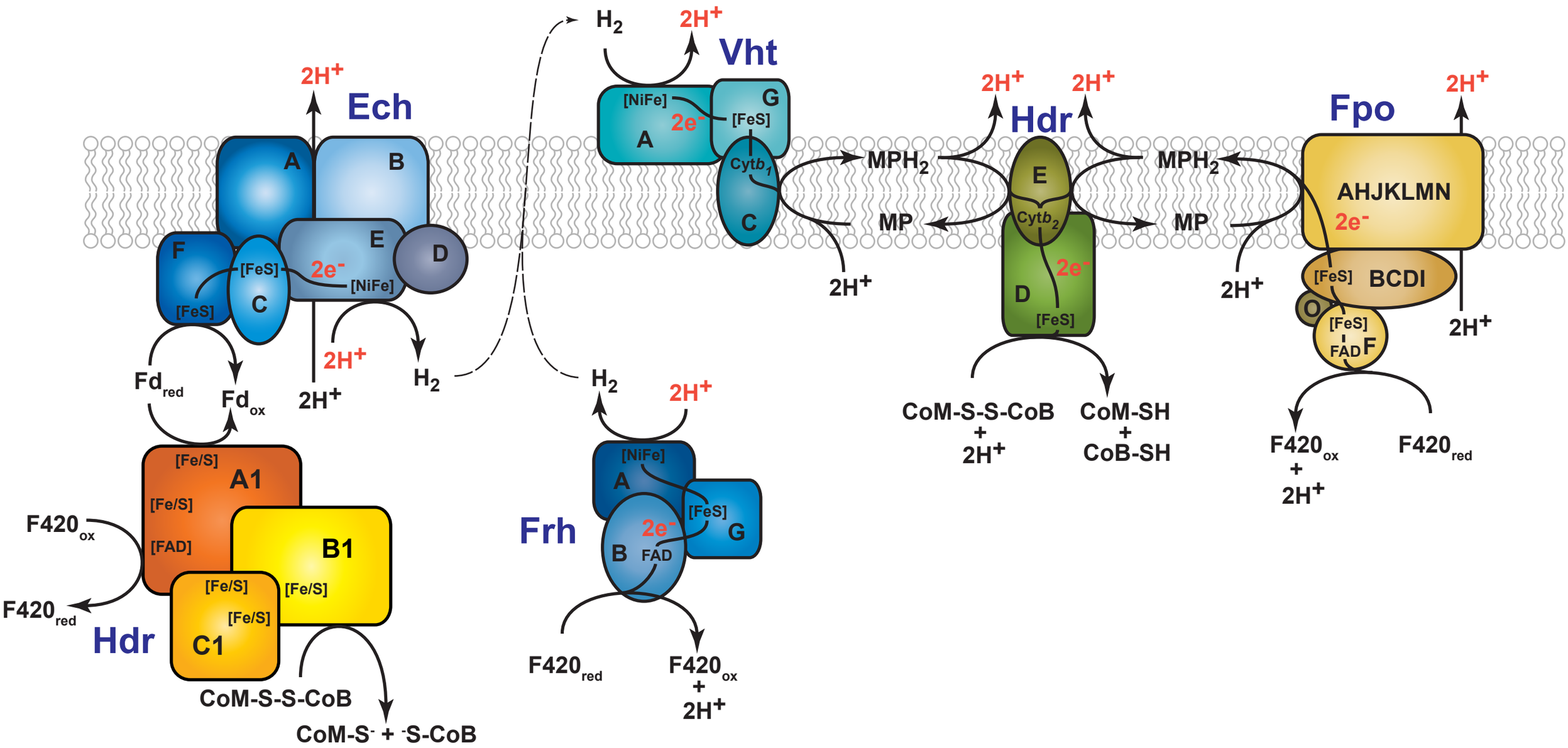

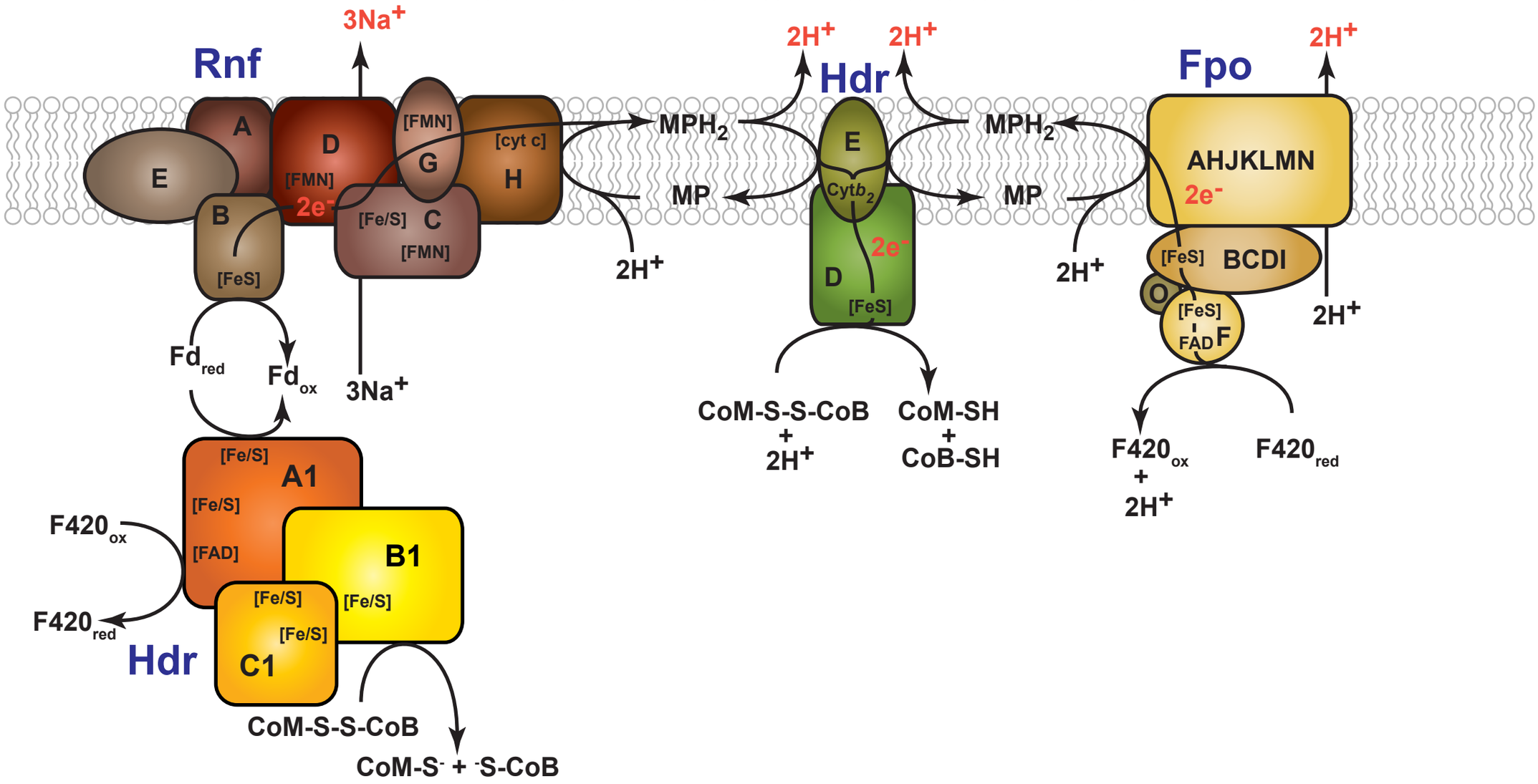

Fig 3. The branched electron transport systems of *Methanosarcina barkeri* and *Methanosarcina acetivorans*. During methylotrophic methanogenesis, *M. barkeri* can utilize H_2-dependent or H_2-independent electron transport systems. The H_2-dependent pathway involves the use of hydrogenases Frh, Ech, and Vht in a H_2 cycling mechanism to transfer electrons from $F420_{red}$ or Fd_{red} to methanophenazine (MP). *M. acetivorans* does not utilize hydrogenases, and is therefore incapable of H_2 cycling. Both organisms can conserve energy via a H_2-independent pathway, wherein electrons are transferred from $F420_{red}$ to MP by way of the F420 dehydrogenase (Fpo). Additionally, the electron transport system in *M. acetivorans i*ncludes the Na^+-translocating Rnf enzyme complex that serves as a Fd:MP oxidoreductase. Both membrane-bound electron transport systems converge at the reduction of the CoM-S-S-CoB heterodisulfide with electrons from reduced MP_{red} via the cytochrome-containing HdrDE enzyme. Protons (or Na^+ in the case of Rnf) are translocated across the cell membrane in both systems, thereby conserving energy in the form of an ion motive force. An additional heterodisulfide reductase, HdrA1B1C1, has been proposed to function in the energy conservation pathways for both organisms. This electron bifurcating enzyme potentially reduces both the CoM-S-S-CoB heterodisulfide and F420 with electrons from Fd_{red} at a stoichiometric ratio of 2 Fd_{red} oxidized for the reduction of 1 CoM-S-S-CoB to CoM-SH/CoB-SH and reduction of 1 $F420_{ox}$ to $F420_{red}$. Abbreviations used are: Fd_{ox}/Fd_{red}, oxidized and reduced ferredoxin; MP/MPH_2, oxidized and reduced methanophenazine; $F420_{ox}$/$F420_{red}$, oxidized and reduced F420; CoM, coenzyme M; CoB, coenzyme B; CoM-S-S-CoB, heterodisulfide of CoM and CoB; FeS, iron-sulfur cluster; FAD, flavin adenine dinucleotide; FMN, flavin mononucleotide; NiFe, nickel-iron active site of hydrogenases; cytb1/cytb2/cyt c, cytochromes.